Cellular Microbiology (2010) **12**(5), 665–676
doi:10.1111/j.1462-5822.2009.01425.x
First published online 10 February 2010

The chemokine-binding protein encoded by the poxvirus orf virus inhibits recruitment of dendritic cells to sites of skin inflammation and migration to peripheral lymph nodes

Zabeen Lateef, Margaret A. Baird,† Lyn M. Wise, Sarah Young, Andrew A. Mercer and Stephen B. Fleming*†
Department of Microbiology and Immunology, University of Otago, PO Box 56, Dunedin, New Zealand.

Summary

Orf virus **(ORFV) is a zoonotic parapoxvirus that induces acute pustular skin lesions in sheep and humans. ORFV can reinfect its host and the discovery of several secreted immune modulatory factors that include a chemokine-binding protein (CBP) may explain this phenomenon. Dendritic cells (DC) are professional antigen presenting cells that induce adaptive immunity and their recruitment to sites of infection in skin and migration to peripheral lymph nodes is critically dependent on inflammatory and constitutive chemokine gradients respectively. Here we examined whether ORFV-CBP could disable these gradients using mouse models. Previously we established that ORFV-CBP bound murine inflammatory chemokines with high affinity and here we show that this binding spectrum extends to constitutive chemokines CCL19 and CCL21. Using cell-based chemotaxis assays, ORFV-CBP inhibited the movement of both immature and mature DC in response to these inflammatory and constitutive chemokines respectively. Moreover in C57BL/6 mice, intradermally injected CBP potently inhibited the recruitment of blood-derived DC to lipopolysaccharide-induced sites of skin inflammation and inhibited the migration of** ***ex vivo*** **CpG-activated DC to inguinal lymph nodes. Finally we showed that ORFV-CBP completely inhibited T responsiveness in the inguinal lymph nodes using intradermally injected DC pulsed with ovalbumin peptide and transfused transgenic T cells.**

Received 13 August, 2009; revised 28 October, 2009; accepted 9 December, 2009. *For correspondence. E-mail stephen.fleming@stonebow.otago.ac.nz; Tel. (+64) 3 479 7727; Fax (+64) 3 479 7744. †Senior authors Margaret Baird and Stephen Fleming have contributed equally to this study.

Introduction

The parapoxvirus, *Orf virus* (ORFV), is a member of the family *Poxviridae* (Fauquet *et al*., 2005). ORFV mainly infects sheep and is readily transmissible to humans (Haig *et al*., 2002). The pathology of ORFV is confined to the epithelium and oral mucosa. The virus usually infects through cuts and abrasions to the skin, and replicates exclusively within keratinocytes (Haig and Mercer, 1998). The resolution of the virus usually takes 4–6 weeks but there have been cases of persistent infection (Savage and Black, 1972; Tan *et al*., 1991; Fleming and Mercer, 2007). ORFV has the ability to reinfect its host, although the lesions are not as severe as for a primary infection and resolve sooner (Haig and McInnes, 2002). The mechanisms underlying this apparent escape from immunity do not appear to involve impaired memory, as a strong delayed-type hypersensitivity reaction to ORFV antigen occurs in previously exposed animals (Buddle and Pulford, 1984; Haig and McInnes, 2002).

Immunity to ORFV infection is characterized by an initial innate inflammatory response that is followed by the development of an acquired immune response (Haig and McInnes, 2002; Haig, 2006). Dendritic cells (DC) that acquire antigen, detect danger signals and subsequently activate naïve T cells are important in this process (Steinman and Banchereau, 2007). DC are actively recruited to the source of infection from blood vessels by a process of extravasation under the influence of inflammatory chemokine gradients (reviewed in Alvarez *et al*., 2008). Upon contact with microorganisms and stimulation with inflammatory cytokines, DC ingest antigens and undergo a process of maturation that involves the upregulation of co-stimulatory molecules and MHC-II. Mature DC then traffic through the afferent lymphatics into the T-cell areas of the peripheral draining lymph nodes following constitutive chemokine gradients to initiate immune responses (Martin-fontecha *et al*.,

2003; Sozzani, 2005; Alvarez *et al.*, 2008). Inflammatory CC chemokines that play a predominant role in the recruitment of DC to sites of infection include CCL2 (MCP-1), CCL3 (MIP-1α) and CCL5 (RANTES) and are produced by the early influx of neutrophils and resident cells (Caux *et al.*, 2000; Diacovo *et al.*, 2005). Immature DC display CCR2 and CCR5 on their surface, which allow these cells to respond to CCL2 and both CCL3 and CCL5 respectively (Alvarez *et al.*, 2008). Constitutive chemokines comprise CCL19 (MIP-3β) and CCL21 (SLC) and are produced from lymph nodes (Martin-fontecha *et al.*, 2003). When DC mature, the inflammatory chemokine receptors are downregulated with a concomitant increase in the receptor CCR7 that allows these mature DC to migrate into lymphoid tissue in response to the constitutive chemokines CCL19 and CCL21 (Dieu *et al.*, 1998; Sallusto *et al.*, 1998; Ohl *et al.*, 2004; Zabel *et al.*, 2005). CCL19 and CCL21 are pivotal molecules for priming T-cell responses, co-stimulating the expansion of naïve CD4+ and CD8+ T cells (Flanagan *et al.*, 2004). CCL21 recruits CCR7+ T cells and DC into the lymph nodes (Ashour *et al.*, 2007) and is involved in the movement of CD4+ T cells within the lymph node (Okada and Cyster, 2007; Worbs *et al.*, 2007). Furthermore CCL21 is upregulated during a febrile response, promoting uptake of lymphocytes across high endothelial venules (Chen *et al.*, 2006).

ORFV has evolved a strategy to subvert the host response by producing secreted factors from virus-infected cells that includes a chemokine-binding protein (CBP) (Seet *et al.*, 2003), a dual-specificity granulocyte macrophage colony-stimulating factor (GM-CSF) and interleukin-2-binding protein (Deane *et al.*, 2000), vascular endothelial growth factor (Lyttle *et al.*, 1994; Savory *et al.*, 2000) and a homologue of interleukin-10 (Fleming *et al.*, 1997; Haig, 2006). These factors are thought to act locally within peripheral tissues at the site of infection. ORFV-CBP is unique in that it has no mammalian homologue and shares low sequence identity (< 17%) to other poxvirus and herpes virus CBPs (Seet *et al.*, 2003). We have previously shown that ORFV strain NZ2 CBP binds a wide range of human CC chemokines, and the C chemokine lymphotactin with high affinity by surface plasmon resonance (Seet *et al.*, 2003). More recently we have shown that it binds a range of murine inflammatory chemokines and inhibits the recruitment of pro-inflammatory monocytes into the infection site (Lateef *et al.*, 2009). Moreover, based on these observations we predicted that ORFV-CBP impairs the recruitment of DC or their precursors from the blood into the skin as well disrupting chemokine gradients that regulate the migration of activated DC to peripheral lymph nodes. We tested this hypothesis using mouse skin models in which purified $ORFV_{NZ2}$-CBP was injected into the dermis of inflamed skin and examined the DC infiltrate at the site of inflammation. In addition, we examined the effects of CBP on mature DC trafficking to peripheral lymph nodes and their ability to stimulate T-cell responses.

Results

CBP binds constitutive chemokines CCL19 and CCL21 with high affinity

Inflammatory chemokines are critical for the recruitment of inflammatory cells to sites of inflammation whereas homeostatic chemokines CCL19 and CCL21 regulate the trafficking of mature DC through the peripheral lymphatics. We have previously reported that $ORFV_{NZ2}$-CBP binds with high affinity to both human and murine inflammatory chemokines CCL2, CCL3 and CCL5, which are the predominant chemokines involved in recruitment of monocyte-derived DC to sites of skin inflammation (Seet *et al.*, 2003; Lateef *et al.*, 2009). Here we investigated the binding affinity of $ORFV_{NZ2}$-CBP-FLAG for murine and human CCL19 and CCL21 using surface plasmon resonance. CBP-FLAG was expressed and purified as previously described (Seet *et al.*, 2003). The CBP-FLAG coupled to the CM5 chip was exposed to murine and human chemokines and monitored as described in *Experimental procedures*. The results are summarized in Table 1. CBP-FLAG bound to murine CCL19 with a KD value of 0.025 nM whereas it bound to murine CCL21 with a much lower affinity with a KD of 7.13 nM. Furthermore, CBP-FLAG was shown to bind to human CCL19 and CCL21 with similar affinities to the murine chemokines (Table 1). The high-affinity interactions are the result of very fast association kinetics ($K_{on} > 10^6\ M^{-1}\ S^{-1}$).

CBP inhibits chemotaxis of DC in response to inflammatory and constitutive chemokines in vitro

The ability of CBP-FLAG to inhibit DC migration in response to the inflammatory chemokines CCL2, CCL3 and CCL5 and constitutive chemokines CCL19 and CCL21 was tested in a transwell migration assay system. DC were generated from the bone marrow of C57BL/6

Table 1. Binding affinity of $ORFV_{NZ2}$-CBP to CCL19 and CCL21.

Chemokines	K_{on} ($\times 10^7$) $M^{-1}\ s^{-1}$	K_{off} ($\times 10^{-3}$) s^{-1}	KD (nM)
mCCL21	0.0235 ± 0.0011	16.7 ± 0.99	7.13
hCCL21	0.086 ± 0.0072	14.7 ± 0.87	1.71
mCCL19	0.136 ± 0.003	0.034 ± 0.005	0.025
hCCL19	0.363 ± 0.004	0.0557 ± 0.0014	0.015

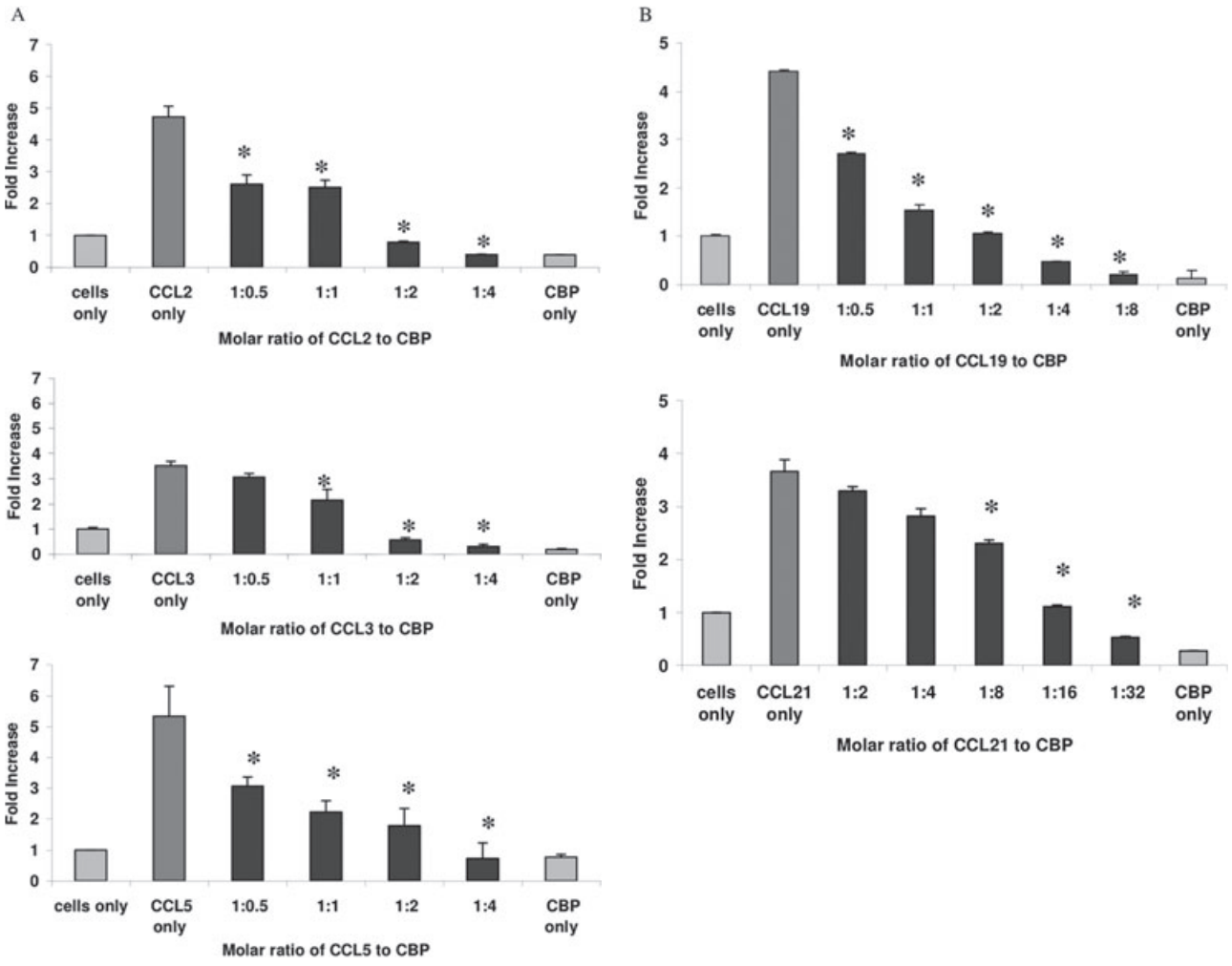

Fig. 1. CBP-FLAG inhibits migration of immature DC in response to inflammatory chemokines and mature DC in response to constitutive chemokines *in vitro*. Chemotaxis assays were performed with a transwell assay system. The inflammatory chemokines CCL2, CCL3 and CCL5 (A) were used at a concentration of 25 ng ml^{-1} and the constitutive chemokines CCL19 and CCL21 (B) were used at a concentration of 12.5 ng ml^{-1}. CBP-FLAG was added to give the molar ratios shown (CCL:CBP). Fold increase represents the migration of DC above the cells only control. The data are shown as mean ± SD of three combined experiments, in which each assay was performed in duplicate. Results significantly different to CCL only ($P < 0.05$; ANOVA, Tukey's test) are indicated by asterisks.

mice in the presence of GM-CSF. By day 5, bone marrow cells were 70% positive for CD11c+, a marker for DC, and displayed an immature phenotype by FACS analysis; MHC-II low, CD80 low, CD86 low, CCR5 high and CCR7 low (Fig. S1). To determine maximal migration of immature DC to inflammatory chemokines, the transwell assay was first optimized for chemokine concentration and time of incubation. The optimum time of incubation was approximately 90 min. DC were most responsive to CCL2 with a sevenfold increase in migration but less responsive to CCL5 and CCL3 with a sixfold and fivefold increase in cell migration respectively (Fig. S2A). The optimal concentration for the chemokines was 25 ng ml^{-1} and this was used in subsequent assays to investigate the effects of CBP on DC migration.

The ability of CBP to block migration of DC in response to CCL2, CCL3 and CCL5 was then tested. Various amounts of CBP-FLAG were added to a constant amount of chemokine in the bottom chamber of a transwell assay and 10^5 DC in a volume of 100 µl were added to the upper chamber. Following a 90 min incubation, cells collected in the bottom chamber were counted using flow cytometry. The CBP-FLAG-reduced chemokine induced migration of DC in a dose-dependent manner (Fig. 1A). The CBP-FLAG was effective at reducing the migration of DC in response to all chemokines tested, even at a molar ratio of chemokine:CBP-FLAG of 1:0.5 for CCL2 and CCL5 ($P < 0.05$, ANOVA Tukey's test) and at molar ratio of 1:1 for CCL3 ($P < 0.05$).

The ability of CBP to block the migration of mature DC in response to CCL19 and CCL21 was then tested. DC were incubated overnight in the presence of CpG and the degree of expression of activation markers on the cell surface analysed flow cytometrically to confirm maturity. CpG-treated DC showed increased expression of MHC-II, CD80 and CD86 (Fig. S1). Importantly these cells showed upregulation of CCR7 and displayed fewer CCR5 markers, compared with cells not exposed to CpG. Mature DC did not respond to CCL3 nor CCL5 (the ligands for CCR5). The optimal concentration of CCL19 and CCL21 to ensure maximal migration of mature DC in the transwell assay was determined to be approximately 12.5 ng ml^{-1} (Fig. S2B). CBP-FLAG inhibited migration in response to both constitutive chemokines in a dose-dependant manner but higher levels of CBP-FLAG were required to produce complete inhibition using CCL21 (molar ratio CCL21:CBP-FLAG 1:32) compared with CCL19 (molar ratio CCL19:CBP-FLAG 1:2) (Fig. 1B).

CBP inhibits the recruitment of DC to inflamed skin

Having established that CBP inhibited cell movement in response to inflammatory chemokines *in vitro*, we next investigated whether CBP could impair the recruitment of DC to inflamed skin using a murine model. The injection of small amounts of LPS into the dermis has been shown to result in highly localized inflammation and a predominant increase in the inflammatory chemokines CCL2, CCL3 and CCL5 (Kopydlowski *et al.*, 1999). In preliminary experiments we determined the optimal levels of LPS to inject into the dermal layer of the abdominal region of C57BL/6 mice and the time at which maximal inflammatory cell recruitment was evident (Fig. S3). Animals were then co-injected with 1 μg of LPS with or without various amounts of CBP-FLAG and 24 h later cells were isolated from excised skin, stained and quantified as described in *Experimental procedures*. Figure 2A shows that 100 ng and 1 ng of CBP-FLAG significantly inhibited recruitment of CD11c+/MHC-II+ DC ($P < 0.01$; paired Student's *t*-test) whereas 0.01 ng of CBP had no affect on recruitment.

We then tested whether CBP could impair recruitment of blood-derived precursor DC to the skin. Bone marrow cells from eGFP transgenic C57BL/6 donor mice were administered to C57BL/6 mice and 24 h later LPS with various concentrations of CBP-FLAG were injected into the dermis of the abdominal region of the recipients. A day later mice were euthanized and skin around the intradermal injection site excised and cells isolated and analysed flow cytometrically. The results show that CBP-FLAG significantly inhibited the recruitment of blood-derived eGFP-DC at 1 ng and 100 ng of CBP-FLAG ($P < 0.01$, Student's *t*-test for paired samples) with the most potent inhibition seen at 100 ng of CBP-FLAG (Fig. 2B). These data suggest that CBP can block chemokines *in vivo* impairing their capacity to attract DC from the blood to the site of inflammation.

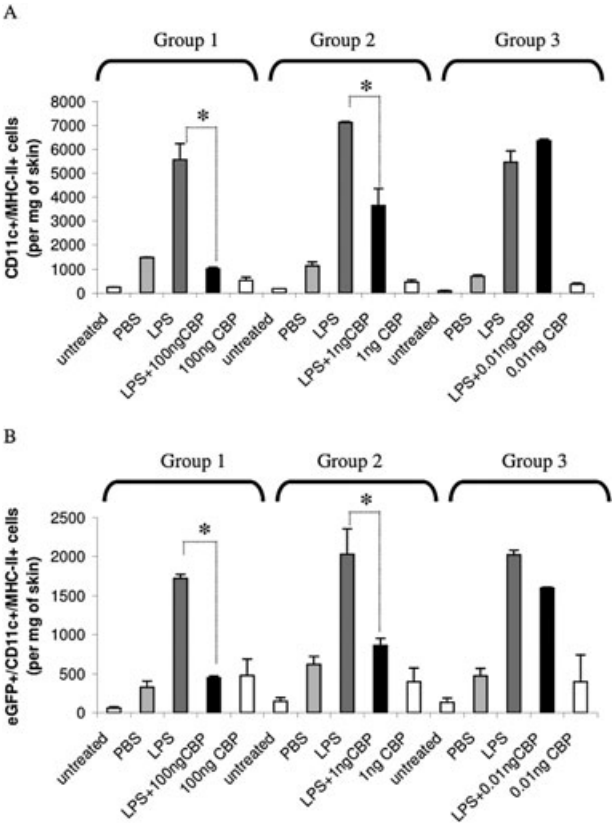

Fig. 2. CBP-FLAG inhibits LPS-induced recruitment of CD11c+/MHC-II+ DC into the skin.
A. Mice received intradermal injections of LPS (1 μg per site) in the abdomen with or without CBP-FLAG. In addition, each mouse received injections of CBP-FLAG only and PBS, i.e. a total of four injections per mouse ($n = 3$ animals per group). Twenty-four hours later mice were euthanized and the skin around the injection sites was excised, weighed and digested to form single-cell suspensions. In addition, cells were prepared in the same manner from untreated skin. Cells were stained for CD11c and MHC-II and counted by flow cytometry.
B. Bone marrow cells from eGFP donor mice were transfused intravenously into recipient mice 24 h before intradermal injection of LPS (1 μg per site) with and without CBP-FLAG as described above and 24 h later the recruitment of eGFP+/MHC II+/CD11c+ cells into the skin sites were analysed.
In both (A) and (B) each bar represents the mean ± SD from three combined experiments. Asterisks indicate results that are significantly different ($P < 0.01$; ANOVA, paired Student's *t*-test).

CBP inhibits the migration of activated DC from the skin to draining lymph nodes

When DC mature, they downregulate their responsiveness to inflammatory chemokines and traffic to the draining lymph node by upregulating the receptor CCR7 that

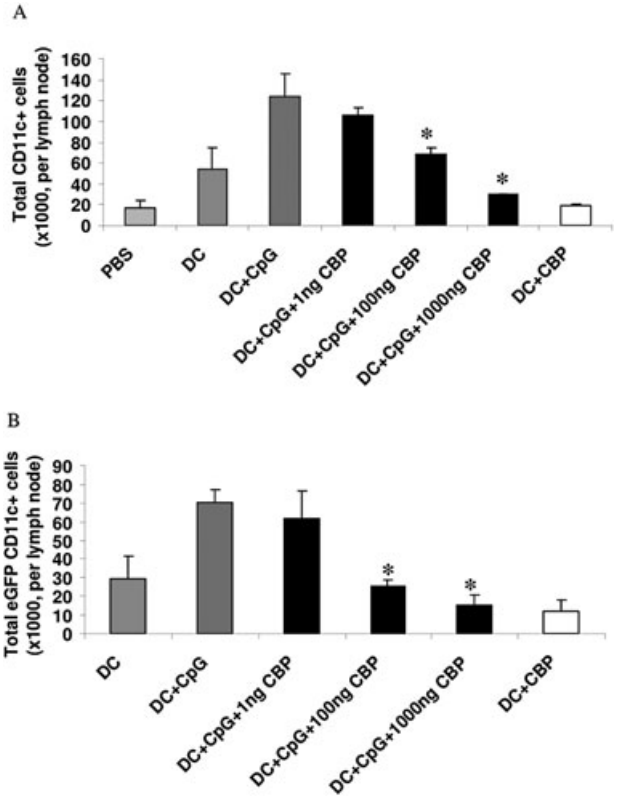

Fig. 3. CBP-FLAG inhibits the migration of mature DC to the draining lymph nodes. Bone marrow-derived DC from eGFP mice were matured with CpG and co-injected intradermally with various concentrations of CBP-FLAG. Each mouse received two injections, one on either side of the abdomen ($n = 3$ animals per group). Twenty-four hours later the draining inguinal lymph nodes were harvested and single-cell suspensions stained for CD11c and analysed flow cytometrically. (A) Total CD11c+ cells; (B) eGFP+/CD11C+ cells in lymph nodes. Each bar represents mean and standard deviation of three combined experiments. Asterisks indicate results that are significantly different ($P < 0.05$; ANOVA, Student's unpaired *t*-test) when compared with the DC + CpG control.

responds to the constitutive chemokines CCL19 and CCL21 (Dieu *et al.*, 1998). The ability of CBP to block CCL19 and CCL21 and thereby impair the migration of DC from the skin to draining lymph nodes *in vivo* was therefore examined. In preliminary experiments DC generated from eGFP mice and activated with CpG were injected into the lower abdomen of mice. Within 24 h a large proportion of these cells had migrated to the inguinal draining lymph nodes (Fig. S4). We then investigated whether or not CBP could block this migration. Various amounts of CBP-FLAG were injected with CpG-treated DC into the lower abdomen. The results show that CBP-FLAG significantly inhibited DC migration at 100 ng ($P < 0.01$) with the most potent inhibition seen at 1 μg (Fig. 3). The data show that CBP is able to block constitutive as well as inflammatory chemokines, thereby impeding the migration of DC to the draining node to initiate an acquired immune response.

CBP blocks T-cell proliferation in the draining lymph node

Since CBP impairs the migration of DC to peripheral lymph nodes, we wished to investigate whether or not this resulted in reduced T-cell responses at the draining lymph node. We used cells from transgenic OT-I and OT-II mice for these experiments.

OT-I mice have CD8+ T cells that respond specifically to the ovalbumin peptide SIINFEKL whereas OT-II mice have cells that respond to ovalbumin (OVA). In preliminary experiments bone marrow-derived DC pulsed with OVA or SIINFEKL were shown to mature (Fig. S5). C57BL/6 mice were adoptively transferred with CSFE-labelled CD8+ T cells from OT-I donor mice. DC pulsed with SIINFEKL were injected intradermally the next day. OT-I CD8 T cells harvested from the inguinal nodes of individual mice that had been injected with DC pulsed with 5 μg ml^{-1} SIINFEKL induced the greatest proliferation (Fig. S6A), so this concentration was used against increasing concentrations of CBP. Co-injection of increasing doses of CBP-FLAG with the pre-pulsed DC resulted in fewer divisions of CD8+ T cells within draining lymph nodes (Fig. 4A). One microgram of CBP inhibited T-cell proliferation by greater than 80%, whereas 100 ng of CBP inhibited proliferation by approximately 50%.

A similar experiment was also carried out with CD4 cells isolated from OT-II transgenic mice that recognize OVA protein (specifically ovalbumin segment 323–339) in the context of MHC-II. In this case the optimal concentration of OVA with which to pulse DC was determined to be 100 μg (Fig. S6B). Again the co-injection of increasing amounts of CBP-FLAG with OVA-treated DC inhibited the proliferation of CD4+ T cells in a dose-dependent manner similar to that described above for CD8+ T cells (Fig. 4B). This shows that CBP introduced into the skin can inhibit antigen-specific T-cell activation within the draining lymph node. This is likely to be attributable to impaired migration of antigen-pulsed DC required to prime naïve T cells.

Discussion

ORFV has evolved to replicate exclusively within keratinocytes of the skin and it encodes a number of virulence factors that interact with immune cells and cytokines within this localized environment that allow it to do this. In this study we asked whether the ORFV-CBP has a role in impairing the development of adaptive immunity by targeting the chemokine gradients that are critical for the recruitment of DC to skin during inflammation and

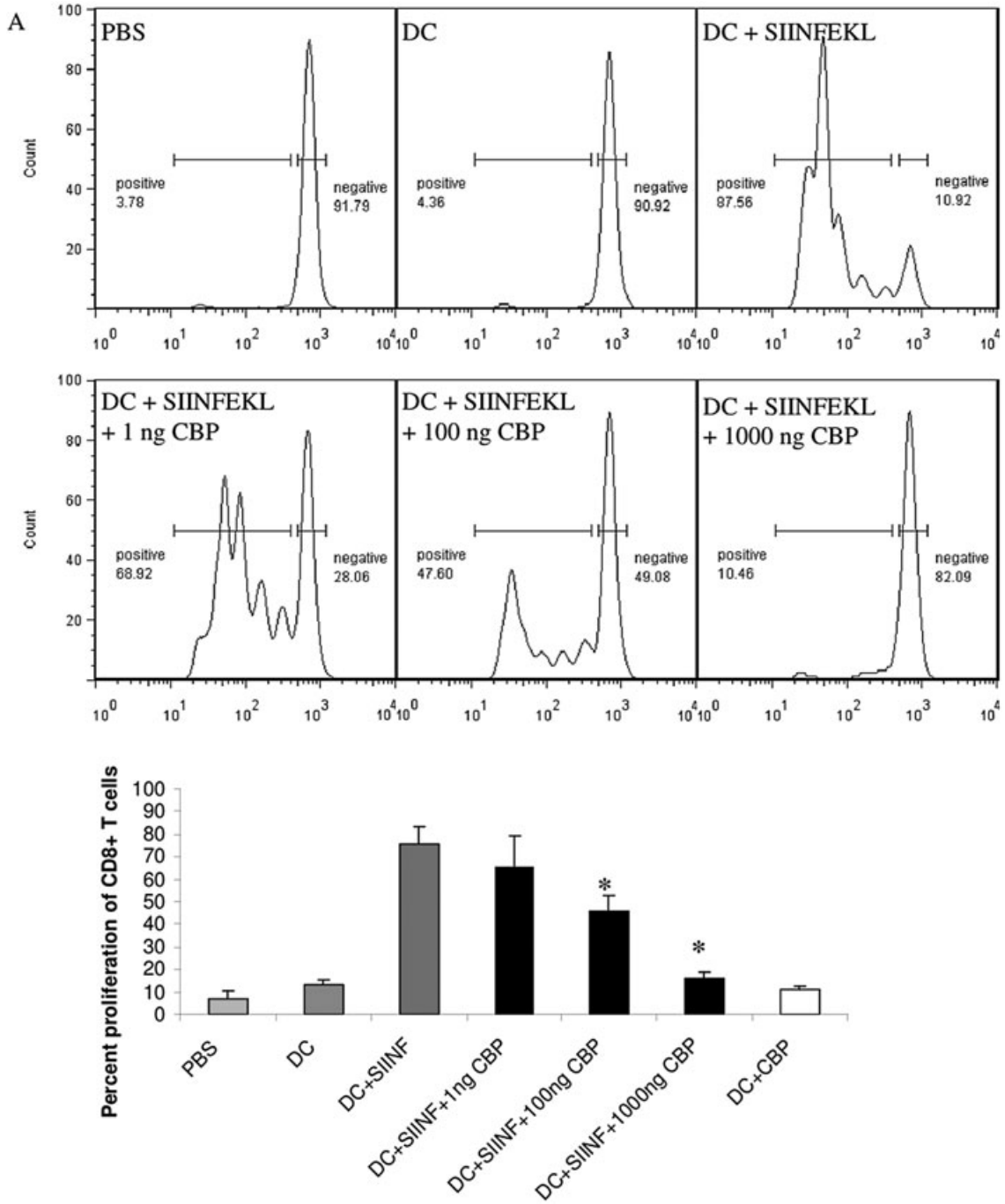

Fig. 4. CBP-FLAG inhibits the proliferation of ovalbumin-specific transgenic T cells following injection of mature DC pulsed with either ovalbumin protein (OVA) or peptide. CFSE-labelled CD8 or CD4 T cells from OT-I or OT-II donors, respectively, were injected intravenously into separate groups of recipients. Twenty-four hours later bone marrow-derived DC pulsed with either SIINFEKL or OVA were co-injected intradermally with or without CBP-FLAG into the abdomen of the CD8+ T-cell recipients (SIINFEKL-pulsed DC) or CD4+ T-cell recipients (OVA-pulsed DC). Control groups were injected with PBS or DC only. Two days later the inguinal nodes were harvested and single-cell suspensions were analysed flow cytometrically for CD8+ or CD4+ CFSE-labelled lymphocytes. FACS histograms of CFSE-labelled cells isolated from a single lymph node are shown; (A) proliferation of CD8+ cells where DC were pulsed with SIINFEKL peptide, (B) proliferation of CD4+ cells where DC were pulsed with OVA. Treatments are shown on the FACS histograms. Per cent T-cell proliferation is shown below the FACS histograms. The degree of proliferation (the number of T cells in which the CFSE label had reduced) was calculated as a percentage of the total number of CFSE-labelled T cells present in each lymph node. Each bar represents mean ± SD of three combined experiments, each with three mice per group. The asterisk (*) denotes significance at $P < 0.05$ ANOVA, Student's unpaired *t*-test, compared with the antigen-pulsed DC control.

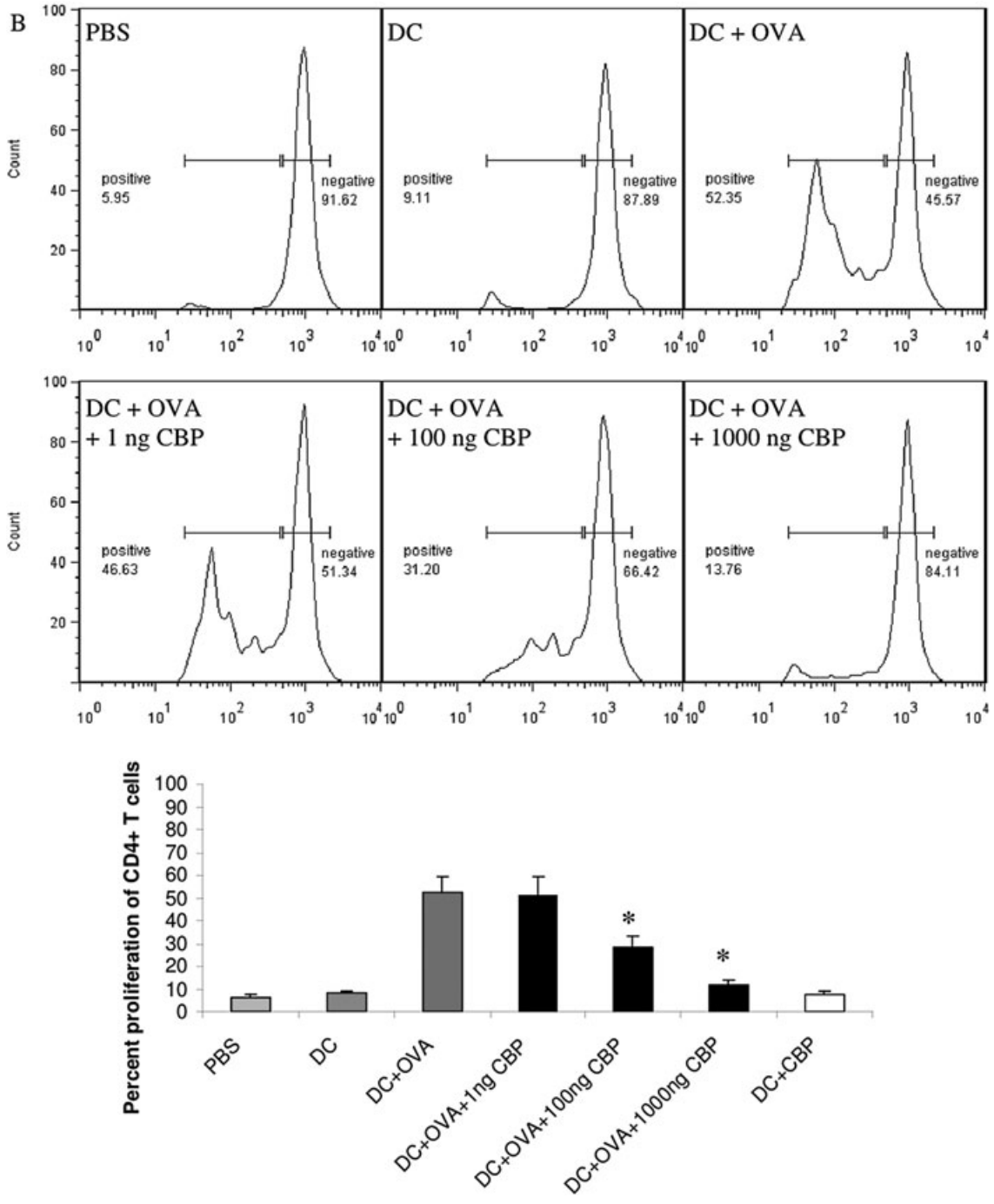

Fig. 4. *cont.*

subsequent trafficking to and within secondary lymphoid tissue. The detailed knowledge of murine immune regulation in conjunction with the availability of reagents for in-depth analyses of chemokine responses in the mouse meant it was desirable to address these questions in murine models. ORFV does not infect mice but we have shown that $ORFV_{NZ2}$-CBP binds to a range of murine chemokines, making mice an appropriate model system in which to study the activities of CBP. Further, the chemokine family forms a large complex network of molecules that are well conserved in structure and function in mammals (Mestas and Hughes, 2004; Zlotnik *et al.*, 2006).

Previous studies have shown that $ORFV_{NZ2}$-CBP binds a range of human and murine inflammatory chemokines (Seet *et al.*, 2003; Lateef *et al.*, 2009) and the results presented here extend this range to include the consti-

tutive chemokines CCL19 and CCL21 for murine and human species. The binding affinity of CBP to CCL19 was several orders of magnitude higher than its binding affinity to CCL21. Chemotaxis assays demonstrated that low levels of CBP could effectively impair murine chemokine-induced migration of both immature and mature DC. The binding affinity of the CBP for both inflammatory and constitutive chemokines was generally reflected in their ability to block migration of DC in response to these molecules in transwell assays. A molar ratio of CBP:chemokine of approximately 4:1 in the case of CCL2, CCL3, CCL5 and CCL19 was sufficient to inhibit approximately all DC migration indicating the potential of this factor to disable chemokine gradients that are critical for DC trafficking *in vivo*. In contrast, we observed that relatively high levels of CBP were required to block mature DC migration in response to CCL21 (32:1) and these levels correlated with its reduced affinity for this chemokine.

The murine models clearly showed that small amounts of CBP (100 ng) were sufficient to inhibit DC recruitment to inflamed skin, but higher levels were required to impair DC migration to the inguinal lymph node. We have estimated that CBP is produced from ORFV-infected cells in culture in the order of 6–120 ng ml^{-1} over 2–4 days (our unpublished data). Such levels of CBP are sufficient to effectively block inflammatory cell recruitment in peripheral tissues based on our findings in this study and previous studies (Lateef *et al*., 2009). However, the levels of CBP required to block DC migration to lymph nodes and T-cell proliferation in the mouse models were substantially greater than the predicted physiological levels in virus-infected tissue. An explanation for the high levels of CBP in this case could involve the reduced ability of CBP to disable the chemokine gradients involved in trafficking of DC to the lymph nodes and to regions within the lymph node in which DC/T cell interactions take place. CCL19 is produced exclusively within the lymph node and directs DC to T-cell zones, whereas CCL21 is produced from the afferent lymphatic ducts and T-cell zones within the lymph node (Martin-fontecha *et al*., 2003; Alvarez *et al*., 2008). In addition to CCL21, other chemokines that are involved in DC migration from peripheral tissues to the lymph node include CCL1 and CXCL12. These factors are required for the migration of DC to the afferent lymphatic endothelium and then a range of factors are required for DC to traverse the endothelium (Alvarez *et al*., 2008). In this study we did not determine whether CBP binds CCL1 or CXCL12. CCL21 is essential for the migration of DC to the lymph node (Ohl *et al*., 2004) and interactions with this chemokine alone would block DC trafficking within the lymphatic endothelium duct. The relatively reduced binding affinity of CBP for CCL21 compared with CCL19 and the inflammatory chemokines may explain the higher levels of CBP required to block DC trafficking in lymphatic tissue which prevented them from reaching the lymph node. Similarly, in transwell assays we observed that it required almost 10-fold more CBP to inhibit migration of DC in response to CCL21 compared with CCL19 and the inflammatory chemokines.

Although CBP shows high binding affinity for CCL19 and CCL21 the question remains whether it is able to enter the parenchyma or high endothelial venules of the lymph node where the CCL19 and CCL21 gradients exist. Low-molecular-weight molecules and chemokines have been shown to enter high endothelial venules from the subcapsular sinus but were excluded from the cortical lymphocyte microenvironments (Gretz *et al*., 2000). The above observations suggest that CBP could potentially disrupt CCL19 and CCL21 gradients within the lymph node. In this study we did not investigate whether CBP was present in the lymph node; however, the fact that eGFP-DC were blocked from entering the lymph node suggests that disruption of CCL19 gradients may be secondary to disruption of CCL21 gradients in the afferent lymphatics. In addition, the infiltration of CBP to various compartments within the lymph node also suggests that CBP could potentially block the movement of blood-derived T cells and B cells that constantly diapedese across high endothelial venules.

Immune mechanisms exist in which T-cell priming is not dependant on the migration of antigen-loaded DC to the lymph node. Soluble free antigen can enter lymph and is processed by lymph node resident DC that initiate early T-cell priming (Kissenpfennig *et al*., 2005; Alvarez *et al*., 2008) thus providing a mechanism by which the host immune system could potentially bypass the effects of ORFV-CBP. However, antigen-bearing skin-derived DC are still required for inducing full-fledged effector responses (Itano *et al*., 2003). In our model it is possible that resident DC were also involved in T-cell responses if in fact free antigen (antigen released from *ex vivo* loaded DC) entered the afferent lymphatics. The finding that CBP at the highest concentration reduced CD8+ and CD4+ proliferation to levels that were only slightly higher than the controls (Fig. 4) suggests that resident DC played a minimal role in T-cell responsiveness.

Although we showed that CBP blocked T-cell activation and proliferation, the most likely interpretation of our data is that CBP acts by disrupting the CCL21 gradient within the afferent lymphatic ducts since mature eGFP-DC injected into the skin were prevented from entering the lymph node. This model is supported by the observation that anti-CCL21 antibody has been shown to block DC trafficking within the afferent lymphatics (Saeki *et al*., 1999). ORFV-CBP has clearly evolved to bind a broad range of inflammatory and constitutive chemokines, although it most likely binds the inflammatory chemokines during ORFV infection. It remains to be established

whether it disrupts CCL21 and CCL19 gradients in ovine species. The evolutionary adaptation of ORFV to its natural host suggests that ORFV-CBP will have a stronger binding affinity for ovine constitutive chemokines than to its murine counterparts. This view is supported by the observation that ORFV-CBP binds human CCL19 and CCL21 with higher affinity than murine CCL19 and CCL21. CCL21 is a target for many viruses that cause persistent infections. Simian and human immunodeficiency viruses (Choi *et al.*, 2003), hepatitis C virus (Nattermann *et al.*, 2006) and murine Y-herpesvirus 68 (Jensen *et al.*, 2003) have evolved different mechanisms to block its activity. The pattern emerging is that ORFV produces several factors that have the ability to target cytokines and cells that are critical for the development of adaptive immunity.

The effects of ORFV-CBP on DC trafficking and T-cell responses suggest that it has therapeutic potential for treatment of inflammatory skin diseases. Chronic skin inflammation is a process where DC are constantly sampling antigen in the skin and migrating to the lymph node where they induce the activation and proliferation of T cells. The T cells travel back to the skin where they release cytokines that induce/maintain the inflammatory condition. The finding that ORFV-CBP can impair both the recruitment of DC to sites of inflammation and the stimulation of T-cell responses by antigen-loaded DC suggests that CBP could break this cycle.

Experimental procedures

Mice

Specific Pathogen Free C57BL/6 mice, eGFP transgenic C57BL/6 mice, OT-I TCR transgenic mice (recognizing OVA segment 257–264) and OT-II TCR transgenic mice (recognizing OVA segment 323–339) were obtained from the University of Otago Animal Facility and used with institutional ethical approval.

Antibodies and recombinant proteins

The following rat anti-murine antibodies and their isotype controls were obtained from BD Pharmingen: anti-CD86 (phycoerythrin conjugated, clone GL1, isotype IgG2a), anti-I-A/I-E (phycoerythrin conjugated, clone M5/114.15.2, isotype IgG2b), anti-CCR5 (phycoerythrin conjugated, clone C34-3448, isotype IgG2c). The hamster anti-mouse CD80 (phycoerythrin conjugated, clone 16-10A1, isotype IgG2) and CD11c (allophycocyanin-conjugated, clone HL3, isotype IgG1) were also from BD Pharmingen. The rat anti-mouse CCR7 primary antibody (clone B4-12, isotype IgG2a) and the goat anti-rat secondary antibody (allophycocyanin-conjugated) were both from R&D Systems. The recombinant murine chemokines GM-CSF, CCL2, CCL3, CCL5, CCL19 and CCL21 were obtained from R&D systems. The ORFV-CBP-FLAG was purified by affinity chromatography using anti-FLAG beads (Sigma-Aldrich, MO, USA) from the supernatant of 293 EBNA cells transfected with pAPEX expressing $ORFV_{NZ2}$-CBP-FLAG as described previously (Seet *et al.*, 2003).

Surface plasmon resonance

The surface of a CM-5 chip was immobilized with approximately 300–400 response units (RU; pg mm^{-2}) of $ORFV_{NZ2}$-CBP-FLAG by standard amine coupling using a Biacore 2000 instrument. All experiments were performed at 25°C with HBS-EP (10 mM Hepes, 150 mM NaCl, 3 mM EDTA, 0.005% polysorbate 20; pH 7.4). The coupled CBP-FLAG was exposed to murine chemokines at a flow rate of 100 µl per minute, at concentrations ranging from 3 nM to 300 nM for the duration of 60 s. Chemokines were allowed to dissociate for 200 s before the surface was regenerated using a mixture of ionic and acidic solutions. The data were analysed using BIAevaluation software using the 1:1 protocol for binding with mass transfer (Lateef *et al.*, 2009).

Generation of DC

Bone marrow-derived DC were cultured from C57BL/6 mice as previously described (Faulkner *et al.*, 2000). Briefly, the tibias and femurs of mice were removed and the ends trimmed to expose bone marrow. The bone marrow cells were suspended in Dulbecco's phosphate-buffered saline (DPBS) with 5% fetal calf serum (FCS; Gibco), and RBC-depleted using pre-warmed ammonium chloride. The bone marrow cells (2×10^6 cells ml^{-1}) were cultured in DMEM (Sigma-Aldrich, MO, USA) supplemented with arginine, aspartate, folic acid, L-glutamine, 0.1 mg ml^{-1} penicillin-streptomycin (Roche Diagnostics, IN, USA), 5% FCS and 20 ng ml^{-1} GM-CSF. Cells were incubated at 37°C with 10% CO_2. On day 3, cells were fed by replacing 3 ml of the supernatant with fresh medium. Immature DC were harvested on day 5. To generate mature DC, these cells were pulsed with 5 µg ml^{-1} CpG overnight and washed three times in PBS before use. The phenotype of both immature and mature cells was analysed using flow cytometric analysis.

Transwell migration assays

Chemotaxis assays were performed with 12-well transwells containing 5 µm membrane inserts (Costar). Chemokines in 600 µl of DMEM containing 5% FCS with or without CBP-FLAG were added to the bottom chamber of the transwells and 10^5 DC in 100 µl of DMEM and 5% FCS were added to the top chamber. The assay was incubated for 90 min, after which time the cells that had collected in the bottom chamber were counted using flow cytometry.

Flow cytometric analysis

This was performed using a FACSCalibur (Becton Dickinson). All flow cytometric data were analysed using CellQuest and FlowJo softwares.

Murine skin inflammation model

C57BL/6 mice received intradermal injections (20 µl total volume) of LPS (*Escherichia coli* derived, Sigma) in the abdominal region. Evans blue dye (2 µl of 1% solution) was mixed in each sample to visualize the rate of diffusion of injected material. A day later, animals were euthanized and the skin around the intradermal

injection site was excised and weighed prior to incubating in collagenase dispase (Roche Diagnostics) for 3 h. The isolated cells were counted using the haemocytometer and stained for cell surface expression of CD11c/MHC-II, with the respective isotype controls. DC recruitment from the blood was also assessed using adoptive transfer of eGFP bone marrow transgenic cells into sex-matched C57BL/6 recipients. Bone marrow was collected from donor mice as described above, suspended in DPBS (without FCS) and 3×10^7 cells were administered to each recipient in a 200 μl volume via the tail vein. Twenty-four hours post adoptive transfer of the eGFP cells inflammation was induced in the skin with LPS as described above. All samples were analysed using flow cytometry counts of 10 000 events, and were normalized to haemocytometer counts and weight of individual skin samples.

DC migration from skin to lymph nodes

Dendritic cells cultured from eGFP mice were matured overnight with 5 μg of CpG and washed and re-suspended in PBS. Cells at a concentration of 10^5 were injected with or without CBP into the lower abdomen of C57BL/6 mice. Twenty-four hours later, the draining inguinal lymph node was extracted and collagenase digested. The total cells from each lymph node were determined using haemocytometer counts. Cells were also stained for CD11c marker and analysed using flow cytometry. For each sample, 200 000 events were counted and data were normalized to haemocytometer counts for each lymph node.

T-cell proliferation in lymph nodes

CD8+ or CD4+T cells were isolated from the spleens and inguinal lymph nodes of donor OT-1 or OT-II mice, respectively, enriched immunomagnetically using antibody-conjugated beads (Milltenyi) with an AUTOMacs System and labelled with carboxyfluoroscein succinomide ester (CFSE) before being injected intravenously (200 μl at a concentration of 2.5×10^7 cells ml^{-1}) into sex-matched C57BL/6 mice. A day later, each mouse adoptively transferred with OT-I CD8 cells received an intradermal injection of DC previously pulsed with SIINFEKL peptide for 3 h, while those adoptively transferred with OT-II CD4 cells received DC previously pulsed with OVA protein overnight. Pulsed DC were washed in PBS prior to injection in 20 μl of PBS in the skin of the lower abdomen. Some groups of mice also received CBP that was co-injected with the pulsed DC. Inguinal lymph nodes were harvested 48 h post injection and CFSE-labelled T cells analysed using flow cytometry. For each sample, dot plots were gated for CFSE-positive cells under the FL1 channel. Live gating was used to acquire 1 000 000 counts of only the CFSE-positive cells.

Statistical analyses

All statistical analyses were performed using the MegaStat suite under Excel. The variance between multiple samples was calculated using ANOVA. For comparisons between two samples, either the Student's paired or unpaired *t*-tests were used, with *P*-values of 0.05 and 0.01 considered significant. All experiments were performed three times and individual data were combined (exceptions are stated in the figure legends).

Acknowledgements

This project was supported by funding from the Health Research Council of New Zealand. Z.L. was supported by a Careers Development Award, Health Research Council of New Zealand. We thank Catherine McCaughan, Michelle Wilson and Nichola Real from the Department of Microbiology and Immunology, University of Otago for expert technical assistance and Fiona Clow (Department of Molecular Medicine and Pathology, University of Auckland) for assistance with Biacore analysis. The OT mice were a gift from Sarah Hook, School of Pharmacy, University of Otago.

References

Alvarez, D., Vollmann, E.H., and von Andrian, U.H. (2008) Mechanisms and consequences of dendritic cell migration. *Immunity* **29:** 325–342.

Ashour, A.E., Turnquist, H.R., Singh, R.K., Talmadge, J.E., and Solheim, J.C. (2007) CCL21-induced immune cell infiltration. *Int Immunopharmacol* **7:** 272–276.

Buddle, B.M., and Pulford, H.D. (1984) Effect of passively-acquired antibodies and vaccination of the immune response to contagious ecthyma virus. *Vet Microbiol* **9:** 515–522.

Caux, C., Ait-Yahia, S., Chemin, K., de Bouteiller, O., Dieu-Nosjean, M.C., Homey, B., *et al.* (2000) Dendritic cell biology and regulation of dendritic cell trafficking by chemokines. *Springer Semin Immunopathol* **22:** 345–369.

Chen, Q., Fisher, D.T., Clancy, K.A., Gauguet, J.M., Wang, W.C., Unger, E., *et al.* (2006) Fever-range thermal stress promotes lymphocyte trafficking across high endothelial venules via an interleukin 6 trans-signaling mechanism. *Nat Immunol* **7:** 1299–1308.

Choi, Y.K., Fallert, B.A., Murphey-Corb, M.A., and Reinhart, T.A. (2003) Simian immunodeficiency virus dramatically alters expression of homeostatic chemokines and dendritic cell markers during infection *in vivo*. *Blood* **101:** 1684–1691.

Deane, D., McInnes, C.J., Percival, A., Wood, A., Thomson, J., Lear, A., *et al.* (2000) Orf virus encodes a novel secreted protein inhibitor of granulocyte-macrophage colony-stimulating factor and interleukin-2. *J Virol* **74:** 1313–1320.

Diacovo, T.G., Blasius, A.L., Mak, T.W., Cella, M., and Colonna, M. (2005) Adhesive mechanisms governing interferon-producing cell recruitment into lymph nodes. *J Exp Med* **202:** 687–696.

Dieu, M.C., Vanbervliet, B., Vicari, A., Bridon, J.M., Oldham, E., Ait-Yahia, S., *et al.* (1998) Selective recruitment of immature and mature dendritic cells by distinct chemokines expressed in different anatomic sites. *J Exp Med* **188:** 373–386.

Faulkner, L., Buchan, G., and Baird, M. (2000) Interleukin-10 does not affect phagocytosis of particulate antigen by bone marrow-derived dendritic cells but does impair antigen presentation. *Immunology* **99:** 523–531.

Fauquet, C.M., Mayo, M.A., Maniloff, U., Desselberger, L.A., and Ball, L.A. (2005) *Virus Taxonomy. Eighth Report of the International Committee on the Taxonomy of Viruses*. London: Acadmic Press, Elservier.

Flanagan, K., Moroziewicz, D., Kwak, H., Horig, H., and Kaufman, H.L. (2004) The lymphoid chemokine CCL21

costimulates naive T cell expansion and Th1 polarization of non-regulatory CD4+ T cells. *Cell Immunol* **231:** 75–84.
Fleming, S.B., McCaughan, C.A., Andrews, A.E., Nash, A.D., and Mercer, A.A. (1997) A homologue of interleukin-10 is encoded by the poxvirus orf virus. *J Virol* **71:** 4857–4861.
Fleming, S.B., and Mercer, A.A. (2007) Genus *Parapoxvirus*. In Poxviruses. Mercer, A.A., Schmidt, A., and Weber, O. (eds). Basel: Birkhaeuser Verlag, pp. 127–165.
Gretz, J.E., Norbury, C.C., Anderson, A.O., Proudfoot, A.E., and Shaw, S. (2000) Lymph-borne chemokines and other low molecular weight molecules reach high endothelial venules via specialized conduits while a functional barrier limits access to the lymphocyte microenvironments in lymph node cortex. *J Exp Med* **192:** 1425–1440.
Haig, D.M. (2006) Orf virus infection and host immunity. *Curr Opin Infect Dis* **19:** 127–131.
Haig, D.M., and McInnes, C.J. (2002) Immunity and counter-immunity during infection with the parapoxvirus orf virus. *Virus Res* **88:** 3–16.
Haig, D.M., and Mercer, A.A. (1998) Ovine diseases. Orf. *Vet Res* **29:** 311–326.
Haig, D.M., Thomson, J., McInnes, C.J., Deane, D.L., Anderson, I.E., McCaughan, C.A., *et al.* (2002) A comparison of the anti-inflammatory and immunostimulatory activities of orf virus and ovine interleukin-10. *Virus Res* **90:** 303–316.
Itano, A.A., McSorley, S.J., Reinhardt, R.L., Ehst, B.D., Ingulli, E., Rudensky, A.Y., and Jenkins, M.K. (2003) Distinct dendritic cell populations sequentially present antigen to CD4 T cells and stimulate different aspects of cell-mediated immunity. *Immunity* **19:** 47–57.
Jensen, K.K., Chen, S.C., Hipkin, R.W., Wiekowski, M.T., Schwarz, M.A., Chou, C.C., *et al.* (2003) Disruption of CCL21-induced chemotaxis *in vitro* and *in vivo* by M3, a chemokine-binding protein encoded by murine gammaherpesvirus 68. *J Virol* **77:** 624–630.
Kissenpfennig, A., Henri, S., Dubois, B., Laplace-Builhe, C., Perrin, P., Romani, N., *et al.* (2005) Dynamics and function of Langerhans cells *in vivo*: dermal dendritic cells colonize lymph node areas distinct from slower migrating Langerhans cells. *Immunity* **22:** 643–654.
Kopydlowski, K.M., Salkowski, C.A., Cody, M.J., van Rooijen, N., Major, J., Hamilton, T.A., and Vogel, S.N. (1999) Regulation of macrophage chemokine expression by lipopolysaccharide *in vitro* and *in vivo*. *J Immunol* **163:** 1537–1544.
Lateef, Z., Baird, M.A., Wise, L.M., Mercer, A.A., and Fleming, S.B. (2009) The orf virus encoded chemokine binding protein is a potent inhibitor of inflammatory monocyte recruitment in a mouse skin model. *J Gen Virol* **90:** 1477–1482.
Lyttle, D.J., Fraser, K.M., Fleming, S.B., Mercer, A.A., and Robinson, A.J. (1994) Homologs of vascular endothelial growth factor are encoded by the poxvirus orf virus. *J Virol* **68:** 84–92.
MartIn-Fontecha, A., Sebastiani, S., Hopken, U.E., Uguccioni, M., Lipp, M., Lanzavecchia, A., and Sallusto, F. (2003) Regulation of dendritic cell migration to the draining lymph node: impact on T lymphocyte traffic and priming. *J Exp Med* **198:** 615–621.
Mestas, J., and Hughes, C.C. (2004) Of mice and not men: differences between mouse and human immunology. *J Immunol* **172:** 2731–2738.
Nattermann, J., Zimmermann, H., Iwan, A., von Lilienfeld-Toal, M., Leifeld, L., Nischalke, H.D., *et al.* (2006) Hepatitis C virus E2 and CD81 interaction may be associated with altered trafficking of dendritic cells in chronic hepatitis C. *Hepatology* **44:** 945–954.
Ohl, L., Mohaupt, M., Czeloth, N., Hintzen, G., Kiafard, Z., Zwirner, J., *et al.* (2004) CCR7 governs skin dendritic cell migration under inflammatory and steady-state conditions. *Immunity* **21:** 279–288.
Okada, T., and Cyster, J.G. (2007) CC chemokine receptor 7 contributes to Gi-dependent T cell motility in the lymph node. *J Immunol* **178:** 2973–2978.
Saeki, H., Moore, A.M., Brown, M.J., and Hwang, S.T. (1999) Cutting edge: secondary lymphoid-tissue chemokine (SLC) and CC chemokine receptor 7 (CCR7) participate in the emigration pathway of mature dendritic cells from the skin to regional lymph nodes. *J Immunol* **162:** 2472–2475.
Sallusto, F., Schaerli, P., Loetscher, P., Schaniel, C., Lenig, D., Mackay, C.R., *et al.* (1998) Rapid and coordinated switch in chemokine receptor expression during dendritic cell maturation. *Eur J Immunol* **28:** 2760–2769.
Savage, J., and Black, M.M. (1972) 'Giant orf' of a finger in a patient with lymphoma. *Proc R Soc Med* **64:** 766–768.
Savory, L.J., Stacker, S.A., Fleming, S.B., Niven, B.E., and Mercer, A.A. (2000) Viral vascular endothelial growth factor plays a critical role in orf virus infection. *J Virol* **74:** 10699–10706.
Seet, B.T., McCaughan, C.A., Handel, T.M., Mercer, A., Brunetti, C., McFadden, G., and Fleming, S.B. (2003) Analysis of an orf virus chemokine-binding protein: shifting ligand specificities among a family of poxvirus viroceptors. *Proc Natl Acad Sci USA* **100:** 15137–15142.
Sozzani, S. (2005) Dendritic cell trafficking: more than just chemokines. *Cytokine Growth Factor Rev* **16:** 581–592.
Steinman, R.M., and Banchereau, J. (2007) Taking dendritic cells into medicine. *Nature* **449:** 419–426.
Tan, S.T., Blake, G.B., and Chambers, S. (1991) Recurrent orf in an immunocompromised host. *Br J Plast Surg* **44:** 465–467.
Worbs, T., Mempel, T.R., Bolter, J., von Andrian, U.H., and Forster, R. (2007) CCR7 ligands stimulate the intranodal motility of T lymphocytes *in vivo*. *J Exp Med* **204:** 489–495.
Zabel, B.A., Silverio, A.M., and Butcher, E.C. (2005) Chemokine-like receptor 1 expression and chemerin-directed chemotaxis distinguish plasmacytoid from myeloid dendritic cells in human blood. *J Immunol* **174:** 244–251.
Zlotnik, A., Yoshie, O., and Nomiyama, H. (2006) The chemokine and chemokine receptor superfamilies and their molecular evolution. *Genome Biol* **7:** 243.

Supporting information

Additional Supporting Information may be found in the online version of this article:

Fig. S1. Flow cytometry analysis of immature and mature DC phenotype. Bone marrow-derived DC (day 6) with or without exposure to CpG were phenotyped flow cytometrically using antibodies to cell surface molecules. Dot plot showing percentage of cells in the culture that are CD11c-positive. Histograms show the expression of MHC-II, CD86, CD80, CCR5, and CCR7

on CD11c+ gated cells. The percentages of positive cells are shown for immature (DC, blue line) and mature (DC + CpG, red line) in each histogram.

Fig. S2. DC migrate in response to chemokines *in vitro*. (A) Various concentrations of the inflammatory chemokines CCL2, CCL3 and CCL5 or (B) constitutive chemokines CCL19, CCL21 were placed in the lower chambers of a transwell plate, and immature (A) or mature bone marrow-derived DC (B) were added to the upper chambers and the assay incubated for 90 min. The number of DC that had migrated to the lower chamber was analysed flow cytometrically and expressed as the fold increase over the number of DC migrating to medium only. Each point on the graph represents the mean ± SD of three repeats, each performed in duplicate.

Fig. S3. DC recruitment in murine skin in response to LPS. DC recruitment was induced in abdominal skin by intradermal injection of LPS (volume 20 μl) or PBS (control). Mice were euthanized post LPS treatment and the skin at the site of injection excised. Cells were isolated by digesting skin with collagenase and dispase, stained for CD11c+ and analysed by flow cytometry (10 000 events were counted per sample).

A. Recruitment of DC as a function of time in response to 1 μg of LPS.

B. Dose–response of DC recruitment by LPS at 24 h post injection. Each bar represents mean ± SD of samples from two mice and is representative of three separate experiments.

Fig. S4. Mature DC migrate to the lymph node *in vivo*. Bone marrow-derived DC from eGFP donors with or without exposure to the maturation signal, CpG, were administered intradermally and the draining inguinal lymph nodes were harvested at 24, 48 or 72 h post injection. Lymph node single-cell suspensions were analysed flow cytometrically for total CD11c+ (A) or eGFP+/CD11c+ (B). Each bar represents the mean ± SD of three mice and is representative of three separate experiments.

Fig. S5. Bone marrow-derived DC pulsed with OVA or SIINFEKL undergo maturation. DC were pulsed with SIINFEKL (A) or OVA for 24 h (B) and their phenotype was compared with that of unpulsed cells using flow cytometric analysis. Cells were stained with antibodies to MHC-II, CD80, CD86, CCR5 and CCR7. Each bar represents the mean fluorescence intensity of one sample, and is representative of five experiments for SIINFEKL-pulsed DC and five experiments for OVA-pulsed DC.

Fig. S6. Adoptively transferred, antigen-pulsed DC induce antigen-specific T-cell proliferation *in vivo*. OTI (A) or OTII (B) TCR transgenic T cells labelled with CFSE were adoptively transferred into recipients intravenously and 24 h later mature bone marrow-derived DC, pulsed with the indicated concentrations of SIINFEKL (A) or OVA (B), were injected intravenously. Forty-eight hours later lymph nodes were harvested and a single-cell suspension was analysed flow cytometrically for proliferation of CFSE-labelled T lymphocytes. The dot plots and histograms are from individual lymph nodes and indicate comparative cycles of cell division as a function of the concentration of SIINFEKL or OVA. The histograms are representative of samples collected from three mice per group, and each experiment was repeated twice.

Please note: Wiley-Blackwell are not responsible for the content or functionality of any supporting materials supplied by the authors. Any queries (other than missing material) should be directed to the corresponding author for the article.